

On the Gas Motion in Close Binary Systems

Søren-Aksel SØRENSEN

*Department of Aeronautical Engineering, Faculty of Engineering
Kyoto University, Kyoto 606*

(Received June 7, 1976)

The motion of the circumstellar gas in close binary systems is studied for systems where the secondary is believed to be a black hole. We treat mass loss from the primary star by overflow through the inner Lagrangian point and by a stellar wind efflux. The flow in these models is discussed and compared with the available observational material. It is, however, found that more comprehensive observations must be made before the final choice can be made between these two means of mass exchange. The possibility, that streams ejected from a circumstellar disk around the black hole reach the far side of the primary star, is briefly discussed.

§ 1. Introduction

The existence of gas streams in close binary systems can be detected by distortions in velocity and light curves and by emission lines in their spectra. The existence of disks, tongues and jets has been recognized in several cases. The streams have attracted renewed attention after the identification of compact X-ray sources with close binary systems. The X-ray emission is believed to originate from the accretion of the streams by a collapsed object.

Studies of the structure of the streams have mainly been performed in two ways. The classical approach is the ballistic approximation in which a fluid particle is treated as a single mass particle and its orbit is studied by Newton's equations of motion. This method is applicable to parts of the streams where pressure forces are negligible and reveals many interesting aspects of the streams.¹⁾ In view of a small mean free path in the streams (~ 50 cm), however, a gas dynamical approach is more appropriate. A case of highly supersonic flow was treated by Biermann²⁾ on the basis of the method of characteristics. Prendergast and Taam³⁾ used a semi-hydrodynamical method in their investigation of U Cep., in which they do not solve the differential equations but simulate a solution of the Boltzmann equation. A first order Fluid-in-Cell type method was used by Sørensen, Matsuda and Sakurai⁴⁾ to discuss general features of the streams.

In the present paper a detailed study is presented of a special class of compact X-ray sources containing Cygnus X-1 and 3U 0900-40. These systems are recognized as close binary systems in which the collapsed companion is likely to be a black hole.^{5), 6)} The source 3U 1700-34 has also been mentioned as a candidate for a black hole.⁷⁾ This identification is, however, not well established and the

system will not be included in the present discussion.

A formulation of the problem will be given in § 2. In § 3, the results of the simulations will be presented both for a case of L1-point overflow and for a case of stellar wind efflux. The possibilities for mass loss from the entire system and the assumption that the gas can reach the far side of the primary star,⁸⁾ after being ejected from the disk around the secondary, are discussed briefly in § 4.

§ 2. Formulation of the problem

2.1 *Characteristics of the HD77581-3U 0900-40 system*

The star identified as a visible companion to the source 3U 0900-40 is a B 0.5 Ia supergiant. Its spectroscopic period is 8.96 days, which is in good agreement with the value found from X-ray eclipses. Mass determinations for this star range from $\sim 15 M_{\odot}$ ⁹⁾ to $\sim 50 M_{\odot}$.⁶⁾ With a mass ratio $\eta = M_2/M_1 = 0.09$ the mass of the secondary star ranges from 1.35 to $4.5 M_{\odot}$ corresponding to these estimates. The lower part of this range does not exceed $3.2 M_{\odot}$ which is presently considered to represent the upper limit for the mass of neutron stars.¹⁰⁾ The most recent study by Zuiderwijk et al.¹¹⁾ finds the mass of the primary to be $30 M_{\odot}$ and the collapsed object ($2.7 M_{\odot}$) could thus be a heavy neutron star. The X-ray source, however, lacks regular pulsations which would result in case the gas was accreting onto a rotating neutron star with a magnetic field.¹²⁾ The observed variations in the X-ray flux are irregular and their time scale is 0.1 sec. This agrees well with what can be expected from an accretion disk around a black hole.¹³⁾

On an evolutionary basis, the mass transport is believed to take place after the primary has filled its Roche lobe. When the star evolves, further matter will be lost as a subsonic stream through the L1-point. The matter subsequently falls onto the black hole where it is accreted. In the present case, however, it is doubtful whether this mechanism operates or not. Evolutionary models by van den Heuvel and De Loore¹⁴⁾ suggest a mass flux as high as $10^{-3} M_{\odot}/\text{year}$ after the primary has filled its Roche limit. This amount exceeds the accretion rate permitted by the critical luminosity.²¹⁾ Therefore, the gas must either be lost from the system (see § 4) or be stored in the disk. The latter possibility, however, ultimately leads to the extinction of the X-ray radiation of the system.^{15), 16)}

Observations of the eccentricity (ε) have further enhanced this difficulty. A determination by Wickramasinghe et al.⁶⁾ yielded $\varepsilon = 0.36$ while Zuiderwijk et al.¹¹⁾ found a smaller value $\varepsilon = 0.22$. Both values are unexpectedly large if the tidal interaction in close binary systems is considered. With an eccentric orbit, the Roche lobe will change its size with phase. If the primary star has evolved to fill its limit, strong variations in the mass flux and consequently also in the X-ray luminosity can then be expected. Variations of this kind has not been observed. This indicates that HD77581 has not yet reached to fill its Roche limit. Its mass loss will then occur not as an L1-point overflow but as a supersonic stellar wind

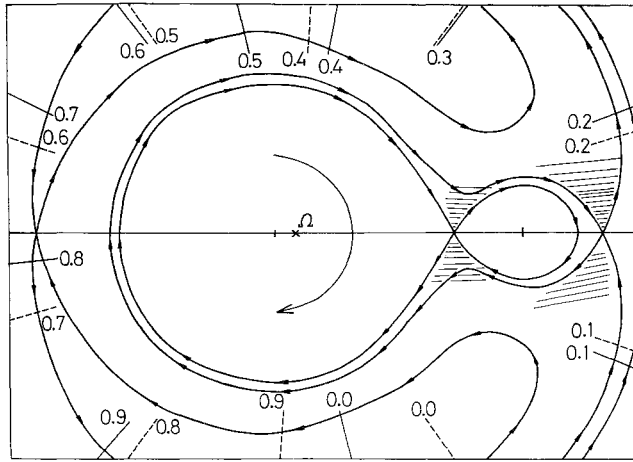


Fig. 1. Schematic diagram of the equipotential surfaces in the HD77581-3U 0900-40 system. Orbital phase is indicated for $\epsilon=0$ (broken) and $\epsilon=0.22$ (solid).

efflux. The detection of the large eccentricity cannot completely rule out the L1-point overflow model. Because the mass ratio (η) is small and the heavy component is the only light source in the system, the amplitude of the velocity curve is small and the variations in the curve may originate from systematic motion in the circumstellar gas as well as from an eccentric orbit. In effect, a recent rediscussion of the light curve of HD77581¹⁷⁾ based on the observations by Jones and Liller¹⁸⁾ has established zero eccentricity for the system. Consequently, there remains the possibility that the transfer of matter can take place through L1-point overflow.

2.2 The HDE226868-Cygnus X-1 system

The primary star in this system is an O 9.7 Iab supergiant with a spectroscopic period of 5.6 days and a mass of $\sim 30 M_{\odot}$.⁵⁾ The estimated mass ratio is $\eta=0.48$ giving a mass of the secondary of $14.4 M_{\odot}$. As a result of a large mass flux, this may be an overestimate.²³⁾ Even if the mass is as low as $10 M_{\odot}$, however, the secondary will exceed the mass limit of a neutron star and must be taken as a strong candidate for a black hole. Because the system is viewed under a small inclination angle ($\sim 30^\circ$), it exhibits no X-ray eclipses but irregular variations on a time scale of 0.05 sec. The eccentricity of the orbit is estimated to be smaller than $\epsilon=0.1$ indicating a circular orbit. Also an estimate of its radius indicates that HDE226868 is filling its Roche limit by more than 90% and there are consequently good reasons to believe that the transfer of matter takes place by means of L1-point overflow. The basic physical structure of the systems is very similar as both have supergiant primaries with a black hole companion, and thus they give an excellent possibility to study the influence on the flow by changes in the orbital elements.

2.3 The model

In the present model the component stars are assumed to have circular orbits and to revolve synchronously around each other with constant angular velocity Ω . The circumstellar gas in the system is assumed to be mono-atomic, ideal and to obey an adiabatic law. The flow is determined by the following equations:

$$\frac{D\mathbf{u}}{Dt} = \mathbf{K} + 2\boldsymbol{\Omega} \times \mathbf{u} - \frac{1}{\rho} \nabla P, \quad (1)$$

$$\frac{DI}{Dt} = -\frac{I}{\rho} \nabla \cdot \mathbf{u}, \quad (2)$$

$$\frac{D\rho}{Dt} = -\rho \nabla \cdot \mathbf{u}, \quad (3)$$

$$P = (\gamma - 1) \rho I, \quad (4)$$

where \mathbf{u} is the velocity, ρ the density, I the specific internal energy, P the pressure and γ the ratio of the specific heats ($=5/3$, here). A Cartesian coordinate system which rotates with the angular velocity Ω is used. The x -axis of this coordinate system coincides with the system axis which connects the centers of the component stars. The combined gravitational and centrifugal force \mathbf{K} is calculated on the basis of the Roche approximation. For non-dimensionalization, the reciprocal of the angular speed is taken as time scale. For technical reasons, a suitably small fraction of the distance between the component stars $\tilde{\mathcal{A}}$ is used as length scale,

$$\begin{aligned} x &= \tilde{x} \mathcal{A} / \tilde{\mathcal{A}}, \\ t &= \tilde{t} \Omega = \tilde{t} [\tilde{G} (\tilde{M}_1 + \tilde{M}_2) (\mathcal{A} / \tilde{\mathcal{A}})^3]^{1/2}, \\ \eta &= \tilde{M}_1 / \tilde{M}_2; \quad \mathbf{K} = \frac{\mathbf{R}_1}{(1 + \eta) R_1^3} + \frac{\eta \mathbf{R}_2}{(1 + \eta) R_2^3} - \mathbf{r}, \end{aligned} \quad (5)$$

where tildes over letters denote dimensional properties and \mathbf{R}_1 , \mathbf{R}_2 and \mathbf{r} are the position vectors from the primary, the secondary and the center-of-mass, respectively. As a density scale, the density on the surface of the primary, which relates to the mass loss rate, is chosen.

§ 3. Calculations and results

Equations (1)~(4) were solved by a time dependent first order Eulerian method for compressible flow.⁴⁾ Like other gas dynamical method, the scheme comprises intrinsic artificial viscosity which stabilized the flow. The artificial viscosity also introduces dissipation, by which the shock waves are smoothed out and an inflow towards the black hole increases. Dissipation can be reduced by the use of a higher order scheme. In the present problem, however, the flow includes the regions in which the flow direction changes rapidly and higher order methods

tend to be locally unstable in these regions. A large amount of artificial viscosity must be added in order to stabilize higher order scheme. In effect, comparative runs clarify that the first order scheme is preferable, in the present problem, to a second order Lax-Wendroff scheme and to the more stable MacCormack scheme.

As to the boundary condition, the edge of the calculation mesh is taken as a free boundary with zero normal derivative. A black hole corresponding to the secondary star is simulated by prescribing zero pressure inside the boundary. The boundary conditions do not take into account the non-adiabatic processes which become important in the innermost parts of the disk and the flow will consequently be fairly insensitive to the mass loss rate. Constant values of the density and the internal energy, respectively, are prescribed on the primary. In systems with L1-point overflow, there is no high coronal temperature to accelerate the gas to supersonic velocities. For a stationary flow, we obtain from (1) and (3)

$$(u^2 - c_s^2) \nabla \cdot \mathbf{u} = u^3 \nabla \cdot \mathbf{i} + \mathbf{u} \cdot \mathbf{K}, \quad (6)$$

where c_s is the local sound speed ($c^2 = dP/d\rho$) and \mathbf{i} is a unit vector in the flow direction. A smooth acceleration through the sonic point is ascertained by $\mathbf{i} \cdot \mathbf{K} = c_s^2 \nabla \cdot \mathbf{i}$. Because $i = \mathcal{A}\Omega \gg c_s$, this condition reduces to $\mathbf{i} \cdot \mathbf{K} \approx 0$. As pointed out by Lubow and Shu,¹¹ therefore, the sonic point is located in the neighbourhood of the L1-point ($K=0$). The velocity on the primary surface is accordingly assumed to have a constant subsonic value except in the neighbourhood of the L1-point at which the sonic velocity is assumed. For systems with a stellar wind where the radius is smaller than the Roche limit, the gas is accelerated to supersonic velocities in the hot corona. Analogously to the situation in a solar wind, the streams are accelerated smoothly across sonic point, as the cross-section of the stream tubes increases outward. Because of the intrinsic artificial viscosity connected with our numerical scheme, however, this process can only be simulated satisfactorily by the use of a fine mesh which leads to a large amount of computer time. The boundary conditions were therefore given on the Roche limit where the radial component of the velocity is assumed to have a constant supersonic value.

In Fig. 2 the resultant flow is shown for the HDE226868-Cygnus X-1 system for a case of L1-point overflow. The mass of the primary is assumed to be $30 M_\odot$, the separation of the component stars to be $47 R_\odot$ and the typical velocity ($\mathcal{A}\Omega$) to be 425 km/sec. For the temperature of the hot O-star, 28,000 °K is assumed corresponding to a sonic velocity of 20 km/sec. The figure shows density contours and velocity vectors in a part of the simulated flow field around the secondary star which is marked by a filled circle. The Lagrangian L1-point is situated on the left edge of the figure and is marked by a cross. The rotation is in the clockwise direction around an axis perpendicular to the plane of the paper.

After leaving the L1-point, the gas is channeled through a narrow stream tube towards the secondary star. As a result of the partial conservation of angular momentum, the gas forms a disk around the star. In the disk, the Coriolis force

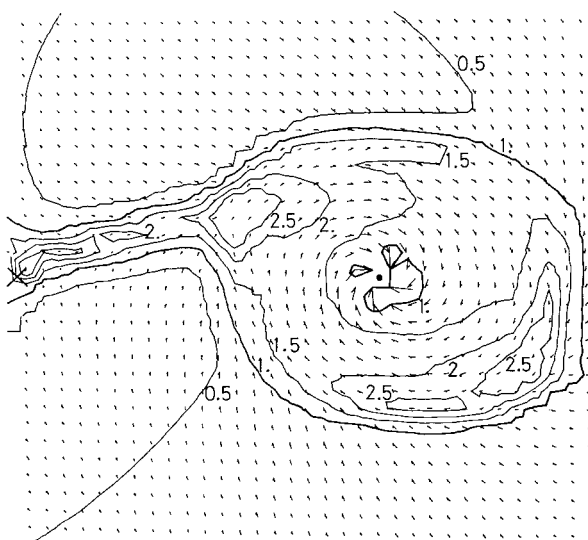


Fig. 2. Density contours and velocity vectors in the HDE226868-Cygnus X-1 system for a case of L1-point overflow.

balances the gravity. Further inwards, the gas motion depends on the efficiency by which the angular momentum is transported outwards. The disk comprises two kinds of shock waves formed on different dynamical reasons. The shock wave in the upper left side of the disk is a usual collision shock formed by the impingement of the mass lost from the L1-point onto the disk. The shocked gas flows along a curved path towards the lower right side of the disk. On its way, the flow has to climb up the potential hill and an oblique shock is formed. This shock is of the same dynamical origin as the shock waves which are identified as the dark lanes of barred galaxies.²⁴⁾ In the inner parts of the disk, the density is seen to decrease. This feature is caused by the influence of the intrinsic artificial viscosity in the computational scheme. The effect is augmented as the resolution of the flow becomes more coarse near the secondary star. The formation of this ring has consequently no physical significance.

In a system in perfect equilibrium the circumstellar flow flows along the equi-potential surfaces.¹⁹⁾ In the present case, however, this assumption cannot be maintained. In areas where the curvature of the equi-potential surfaces is large, the circumstellar gas crosses freely over the equi-potential surfaces and eventually collides with the disk. This causes another collision shock wave which sheathes round the inlet part of the L1-point outflow and appears on the lower part of the disk. The circumstellar gas, however, has only a small amount of total energy and will have little influence on the high energetic flow in the disk. These bounding shock waves around the disk are clearly seen in Fig. 3.

In Figs. 4 and 5 the flow is shown for the case of L1-point overflow in the

HD77581-3U 0900-40 system. The mass of the primary is assumed to be $30 M_{\odot}$. A circular orbit with a period of $8.^d95$ is assumed. The separation of the components will then be $58 R_{\odot}$. The temperature at the primary surface is assumed to be $28,000^{\circ}\text{K}$. The general trend of the flow configuration is the same as that in Fig. 2. Because the star has a smaller mass, however, the effect of Coriolis force becomes more important relative to that of the gravity force of the secondary. The radius of the disk, therefore, increases in comparison to that in previous cases.

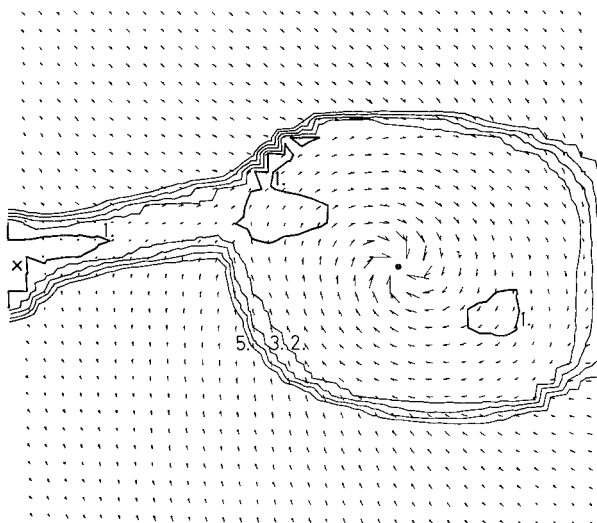


Fig. 3. Mach no. contours for the flow in Fig. 2.

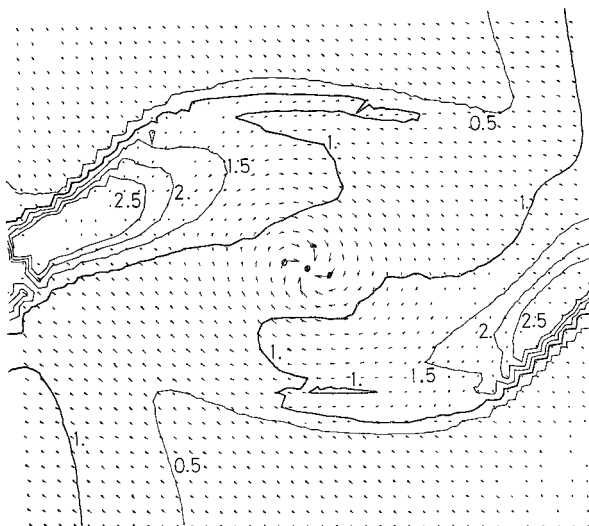


Fig. 4. Density contours and velocity vectors in the HD77581-3U 0900-40 system for a case of L1-point overflow.

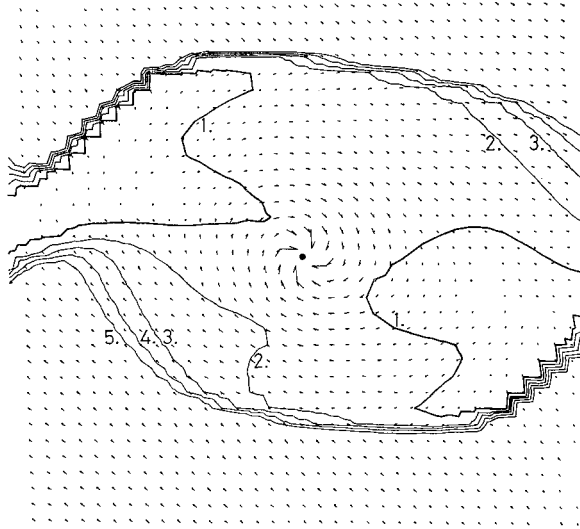


Fig. 5. Mach no. contours for the flow in Fig. 4.

The stream from the L1-point collides with the disk closer to the L1-point and the shock waves come nearer to the primary surface. There also appears a looped tongue from the L1-point as a manifestation of the stronger effect of Coriolis force. The shock on the lower right side of the secondary is also strengthened.

Figures 6 and 7 show the HDE226868–Cygnus X-1 system for a case of stellar wind. Parameters used here are the same as those which were assumed in Figs. 4

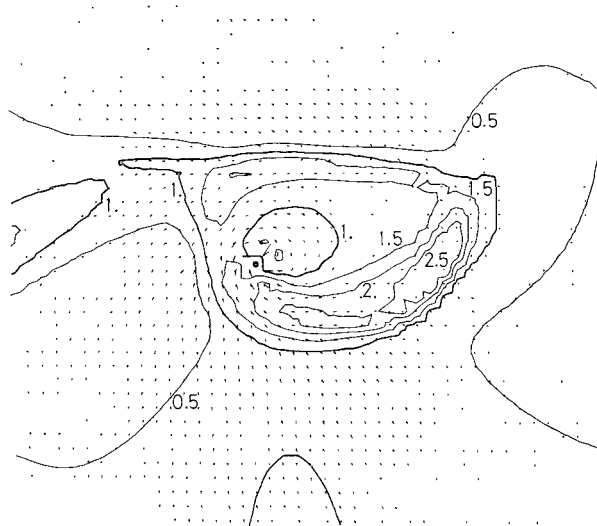


Fig. 6. Density contours and velocity vectors in the HDE226868–Cygnus X-1 system for a case of supersonic stellar wind efflux.

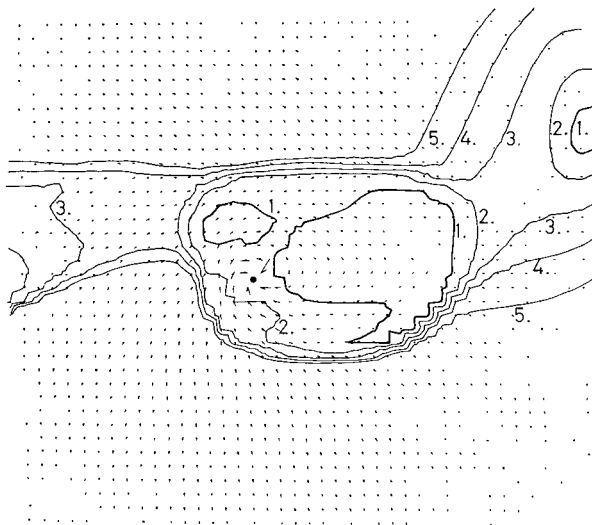


Fig. 7. Mach no. contours for the flow in Fig. 6.

and 5 except that the outflow velocity at the primary boundary is 200 km/sec. This corresponds to a low supersonic state and is approximately 50% of the typical velocity. The balance between the Coriolis force and the gravity manifests itself as a clearly defined disk. Only the circumstellar disk here is strongly asymmetrical with respect to the star. In effect, a large subsonic region is formed behind the star as a result of a shock caused by a crossing over of stream lines across potential lines. The accretion onto the star is also seen to be asymmetrical and the flow can be considered as an intermediate case between the disk formation in Fig. 2 and the infall through an accretion column in Fig. 8.

In Figs. 8 and 9 the HD77581-3U 0900-40 system is shown for a case of stellar wind efflux. Parameters are the same as those which are assumed for the L1-overflow model except for 200 km/sec radial outflow from the primary surface. Because the gravity of the secondary does not effectively bend the outflow, in this case, the formation of a disk becomes impossible. Instead a tail shock is formed behind the star. As is clearly seen in Fig. 9, a subsonic accretion column is formed here. A high density region extends from the leading disk of the primary surface near the L1-point to the secondary star. This region is formed because the gas, here under the influence of both the Coriolis force and the gravity, is bent strongly towards the star. The tilt of the above tail shocks and accretion column can be understood by the impingement of this tilted bridge onto the secondary star.

In order for a black hole to emit X-rays the time scale of radiative cooling and heating for the accreted matter must be short compared with the infall time. Therefore radial accretion cannot give rise to the observed radiation²⁰⁾ but an

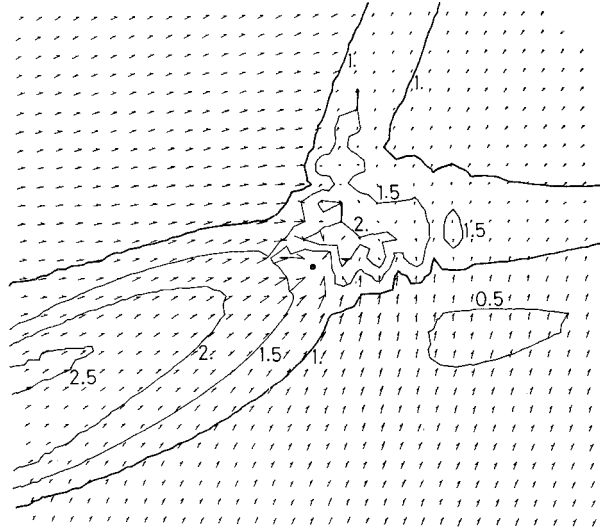


Fig. 8. Density contours and velocity vectors in the HD77581-3U 0900-40 system for a case of supersonic stellar wind efflux.

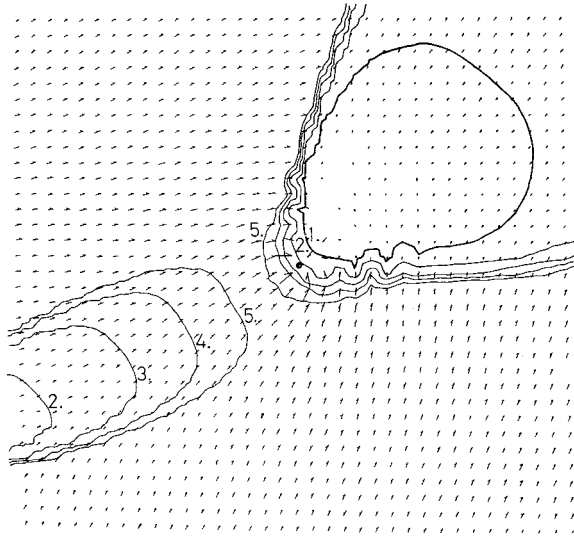


Fig. 9. Mach no. contours for the flow in Fig. 8.

accretion disk must be present around the hole.²¹⁾ Because the gas in the accretion column in this case is always supersonic relative to the main flow, a constant loss of angular momentum will result and no disk can be formed.

In Fig. 10, the observed outflow velocity from HD77581 is plotted against the orbital phase. The orbital phase is shown in Fig. 1 in which dashed lines corresponds to a circular orbit and solid lines to an orbit with an eccentricity of

$\varepsilon = 0.33$. The velocity is found as the difference between radial velocities based on the H_β -line and the velocity based on the higher Balmer lines, and the data are taken from the observations by Zuiderwijk.¹¹⁾ The velocity changes significantly with the orbital phase and the minimum and the maximum appear at orbital phases of 0.1 and 0.4, respectively. A comparison with Fig. 8 clarifies that this flow field agrees best with the general trend of the observed velocity variation. The above result suggests a possibility that the secondary star of HD 77581-3U 0900-40 is a neutron star. However, because a rotating neutron star with magnetic field, must show regular variation of X-ray luminosity in contrast to the observed irregular variation, this identification is not conclusive.

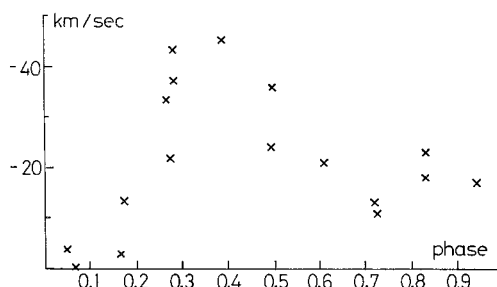


Fig. 10. Observed variations in the outflow velocity at HD 77581 as a function of orbital phase.

§ 4. Irregular streams

In their rediscussion of the orbit for HD 77581, Wickramasinghe and Bessell⁹⁾ found that the star failed to recover brightness following the secondary minimum on March 5th, 1973. The explanation of the incident as obscuration in the orbital plane led Wickramasinghe²²⁾ to suggest that radiation pressure from soft X-rays (with energy smaller than 1 KeV) could cause matter to be ejected from the outer parts of the disk and eventually to reach the far side of the primary. The effect of radiation pressure is clearly of a three-dimensional character because the thickness of the disk increases with distance from the black hole. In order to study the gas dynamical aspects of the problem, however, a simplified model was used. The boundary of the secondary star is replaced by a circle with prescribed radius. The effect of the radiation pressure, which operates inside this boundary to push out the accreting gas, is simulated by a prescribed outward velocity on this boundary. Models with this boundary condition were run in order to check the resulting flow. Based on technical reasons, the calculation is performed piecewise. Therefore, we do not give any unified figure of the flow field as a whole. The main trend of the flow field, however, can be obtained by an inspection of the above piecewise results. Discussion of the flow field thus obtained is given in the following.

In the case of the L1-point overflow, it was found that the gas did not fall back on the primary star for low velocities at the secondary boundary. Instead, a mass loss through the Lagrangian L2-point takes place. This mass is lost from the system and form an expanding cloud around the system. This process is interesting in relation to the mass loss rate from the primary star. If the star

loses mass of the order of $10^{-8}M_{\odot}/\text{year}$ as proposed by van den Heuvel and De Loore¹⁴⁾ for L1-point overflow and all of the mass accretes onto the secondary star, the X-ray source would quickly be extinguished because of a strong self-absorption.

Let us assume that the main part of the above $10^{-8}M_{\odot}/\text{year}$ is stored in a ring outside our boundary near the secondary star and that $10^{-6}M_{\odot}/\text{year}$ accretes onto the black hole. The X-ray radiation localized in the narrow proximity of the black hole is retained. The inner face of the above-mentioned ring is continuously heated by this X-ray and acquires thermal energy. If the amount of this energy exceeds a certain threshold value, this ring is blown off as a geyser blows up intermittently. Because the time scale of our flow field is short compared with the time scale of this blowing up, our present model can be taken as a simulation of the above intermittent process. As is expected, this process influences only the “outer” ring around a black hole.

For high velocities on the secondary boundary, the gas was found to stream back towards the primary surface. The part of the streams which moves direct in the rotational frame was found to be able to reach the far side of the primary. No cases, however, were found in which the gas streams collide on the far side of the primary as was suggested by Wickramasinghe.²²⁾ It seems more probable that the variable minimum in HDE226868 originates from a different source. We propose a condensation of mass lost through the Lagrangian L2-point as an alternative possibility.

§ 5. Concluding remarks

A detailed study of the flow in the close binary systems HDE226868–Cygnus X-1 and HD77581–3U 0900-40 has been presented both for a case of sonic L1-point overflow and a case of stellar wind efflux. From these results, attempts were made to distinguish between these two types of mass exchange. In the case of Cygnus X-1, the secondary component is likely to be a black hole because of its large mass. For this system, however, disk formation is derived even for the case with stellar wind efflux, the initial velocity of which is 200 km/sec. A clear distinction between the two cases, therefore, is not to be made here. Also in the case of 3U 0900-40, a distinction between the two types of flows is difficult. For the case of supersonic efflux, the effluxed matter is accreted through an accretion column instead of through a disk. There is a possibility that the secondary is a neutron star because the mass ranges around the limit for neutron stars. In effect, the flow structure of the system resembles that of Cygnus X-3: The calculated velocity variations fit well with the observed velocity variation, vs, phase found for HD77581. Accretion by a neutron star through an accretion column, however, is expected to exhibit regular pulsations in the X-ray emission. Because no such regular variations have yet been detected, the above identification is not

conclusive.

In order to discriminate between the different types of flow fields, more observational material must be collected. A better determination of the orbit and more accurate mapping of the line of sight velocity, vs. phase are urgently desired. The formation of two shock waves in the disk might also be detected.

Acknowledgements

The author would like to express his gratitude to Professor C. Hayashi and Professor T. Sakurai for their interest and helpful advice. The numerical calculations were performed at the Data Processing Center of Kyoto University and partly at the Institute for Plasma Physics at Nagoya University. The author wants to thank Prof. K. Takayama for placing the computer facilities of the Plasma Institute at his disposal. This work was supported partly by the Japan Society for the Promotion of Science.

References

- 1) S. H. Lubow and F. H. Shu, *Astrophys. J.* **198** (1975), 383.
- 2) P. Biermann, *Astron. Astrophys.* **10** (1971), 205.
- 3) K. H. Prendergast and R. E. Taam, *Astrophys. J.* **189** (1974), 125.
- 4) S. A. Sørensen, T. Matsuda and T. Sakurai, *Astrophys. Space Sci.* **33** (1975), 465.
- 5) C. T. Bolton, *Nature Phys. Sci.* **240** (1972), 124.
- 6) D. T. Wickramasinghe, N. V. Vidal, M. S. Bessell, B. A. Peterson and M. E. Perry, *Astrophys. J.* **188** (1972), 167.
- 7) M. S. Bessell, B. A. Peterson, D. T. Wickramasinghe and N. V. Vidal, *Astrophys. J.* **187** (1974), 355.
- 8) D. T. Wickramasinghe and M. S. Bessell, *Nature* **251** (1974), 25.
- 9) W. A. Hiltner, J. Werner and P. Osmer, *Astrophys. J. Letters* **175** (1972), L19.
- 10) R. W. Leach and R. Ruffini, *Astrophys. J. Letters* **180** (1973), L15.
- 11) E. J. Zuiderwijk, E. P. J. van den Heuvel and G. Hensberge, *Astron. Astrophys.* **35** (1974), 353.
- 12) K. Davidson and J. Ostriker, *Astrophys. J.* **179** (1973), 585.
- 13) R. A. Sunyaev, *Soviet Astron.—AJ* **16** (1973), 941.
- 14) E. P. J. van den Heuvel and C. De Loore, *Astron. Astrophys.* **25** (1973), 387.
- 15) J. E. Pringle, *Nature Phys. Sci.* **243** (1973), 90.
- 16) N. I. Shakura and R. A. Sunyaev, *Astron. Astrophys.* **24** (1973), 337.
- 17) D. T. Wickramasinghe and J. Whelan, *Mon. Not. R. Astr. Soc.* **167** (1974), 21.
- 18) C. Jones and W. Liller, *Astrophys. J. Letters* **184** (1973), L121.
- 19) K. H. Prendergast, *Astrophys. J.* **132** (1960), 162.
- 20) S. Shapiro, *Astrophys. J.* **180** (1973), 531.
- 21) J. Pringle and M. Rees, *Astron. Astrophys.* **21** (1972), 1.
- 22) D. T. Wickramasinghe, *Mon. Not. R. Astr. Soc.* **168** (1974), 297.
- 23) E. P. J. van den Heuvel and J. P. Ostriker, *Nature Phys. Sci.* **245** (1973), 99.
- 24) S. A. Sørensen, T. Matsuda and M. Fujimoto, *Astrophys. Space Sci.* **43** (1976), 491.